

Interaction of ICAM-1 with β 2-integrin CD11c/CD18: Characterization of a peptide ligand that mimics a putative binding site on domain D4 of ICAM-1

Christoph Frick¹, Alex Odermatt*¹, Ke Zen², Kenneth J. Mandell², Heather Edens², Reto Portmann³, Luca Mazzucchelli⁴, David L. Jaye² and Charles A. Parkos*²

¹ Department of Nephrology and Hypertension, Department of Clinical Research, University of Berne, Berne, Switzerland

² Epithelial Pathobiology Research Unit, Department of Pathology and Laboratory Medicine, Emory University, Atlanta, GA, USA

³ Friedrich Miescher Research Institute, Basel, Switzerland

⁴ Institute of Pathology, Locarno, Switzerland

The integrin CD11c/CD18 plays a role in leukocyte and cell matrix adhesion and is highly expressed in certain hematopoietic malignancies. To better characterize ligand binding properties, we panned random peptide phage-display libraries over purified CD11c/CD18. We identified a phage expressing the circular peptide C-GRWSGWPADL-C. C-GRWSGWPADL-C phage bound specifically to CD11c/CD18 expressing monocytes but not CD11c/CD18 negative lymphocytes and showed 5×10^3 -fold higher binding to purified CD11c/CD18 than control phage, without binding to CD11b/CD18. Peptide sequence analysis revealed a similar sequence in domain D5 of ICAM-1 and an alternative, phase-shifted motif in domain D4. Surface plasmon resonance experiments demonstrated direct interaction of ICAM-1 and CD11c/CD18. A soluble fusion protein containing the extracellular domain of ICAM-1 abolished C-GRWSGWPADL-C phage binding to CD11c/CD18. Moreover, synthetic monomeric circular peptide C-GRWSGWPADL-C bound specifically to CD11c/CD18 and inhibited ICAM-1 binding. Its rather low binding affinity and inability to displace pentavalent C-GRWSGWPADL-C phage from CD11c/CD18 suggests that a multimeric display of the selected peptide is essential for high affinity binding. Using ICAM-1 deletion constructs, we showed that domain D4 is required for interaction with CD11c/CD18, suggesting that C-GRWSGWPADL-C phage binds specifically to CD11c/CD18 by structurally mimicking the interaction site on D4 of ICAM-1.

Received 6/12/04

Revised 14/8/05

Accepted 30/9/05

[DOI 10.1002/eji.200425914]

Key words:

ICAM-1 · Integrin
 · Peptide ligand
 · Phage-display

* A.O. and C.A.P. had equal responsibilities in the planning and execution of this work.

Correspondence: Dr. Alex Odermatt, Department of Nephrology and Hypertension, Department of Clinical Research, University of Berne, Freiburgstrasse 15, 3010 Berne, Switzerland
 Fax: +41-31-632-9444

e-mail: alex.odermatt@dkf.unibe.ch

Abbreviations: ICAM-1: intercellular adhesion molecule-1 ·

TU: transducing units

Introduction

β 2-Integrins are expressed exclusively on leukocytes and play a key role in leukocyte adhesion to the endothelium and subsequent transmigration through interactions with molecules expressed on the surface of endothelial cells, including ICAM-1. These heterodimeric adhesion molecules consist of a common β -subunit (CD18) that associates with one of four α -subunits, CD11a (LFA-1), CD11b (Mac-1), CD11c (p150) or CD11d [1]. A majority of the ligand binding properties of β 2-integrins are

mediated through interactions with a 200 amino acid inserted or I-domain present within the extracellular domain of the α -subunits [2, 3]. For ligand binding, the I-domain must be activated by a conformational change [4]. Changes in tertiary conformation of β 2-integrins allow regulation between active and inactive conformations by accessibility of the metal ion-dependent adhesion site [5].

CD11b and CD11c are closely related proteins sharing 63% amino acid homology [6]. Many ligands have been described for CD11b/CD18, including iC3b [7], fibrinogen [8], heparin [9], elastase [10], JAM-C [11, 12] as well as the important adhesion molecules ICAM-1 [2], ICAM-2 [13] and ICAM-4 [3, 14]; however, much less is known about CD11c/CD18. Many approaches have been taken by investigators to identify ligands for these integrins, including random peptide phage-display. Ruoslahti and coworkers [15] have applied phage-display to screen peptide libraries for ligands binding to purified integrins as well as to intact cells expressing integrins. These screenings often resulted in the selection of peptide ligands containing a conserved RGD-motif, which mediates binding to $\alpha_5\beta_1$, $\alpha_v\beta_3$, $\alpha_v\beta_5$, and $\alpha_{IIb}\beta_3$ integrins. However, the RGD-motif is not a required feature in ligands for β 2-integrins [5].

Recently, using peptide phage-display technology, Koivunen *et al.* [16] identified a peptide LLG-C4, binding to CD11a/CD18. At millimolar concentrations, this peptide inhibited CD11a-mediated leukocyte cell adhesion to ICAM-1, indicating that it may structurally mimic the first domain of ICAM-1, which mediates binding to CD11a/CD18 [17]. Additional evidence for the importance of interaction of β 2-integrins with ICAM-1 was provided by Diamond *et al.* [18] demonstrating interaction of CD11b/CD18 with the third domain of ICAM-1. It was also suggested that CD11c/CD18 may act as a ligand for ICAM-1 [2, 19], although direct interaction between these two proteins has never been demonstrated.

Despite these reports, little is known about ligand binding and functional specificity of CD11c/CD18. To gain further insights into potential binding partners for CD11c/CD18, we employed random peptide phage-

display taking advantage of the ability to purify functional CD11c/CD18 from human cells. We describe a peptide ligand that binds specifically to CD11c/CD18. We also show that ICAM-1 directly binds to CD11c/CD18 and provide evidence that the selected motif mimics the binding site in domain D4 on ICAM-1. The structural information gained from this study as well as the peptide reagents generated may lead to better strategies for manipulating ICAM-1- β 2-integrin interactions for experimental and therapeutic purposes.

Results

Selection of C-GRWSGWPADL-C phage specifically binding to CD11c/CD18

To identify CD11c/CD18-specific peptide ligands, the circular decapeptide library CL10 and the linear nonapeptide library LL9 were screened using CD11c/CD18 purified from splenic tissue removed during treatment of a patient with hairy cell leukemia. Biopanning experiments were performed using purified integrin coated onto polysorb microtiter plate wells. Two independent panning experiments, using coated CD11c/CD18 and the circular library CL10, yielded exclusively phage with the sequence C-GRWSGWPADL-C (N1) (Table 1). The phage was eluted with low pH. Sequencing phage after the fourth round of panning did not yield C-GRWSGWPADL-C phage or phage containing a partial motif. In a third independent experiment with library CL10 and CD11c/CD18, after four rounds upon elution with EDTA-containing buffer, five out of ten sequenced phage displayed the circular peptide C-HKGHDRGKCR-C (P8).

Similar experiments performed with immobilized purified CD11b/CD18 did not result in the selection of a single peptide motif. Phage bearing linear peptides with the consensus MDKXH were selected at increased frequency. Elution of phage with functional anti-CD11b/CD18 antibody CBRM1/29, instead of using low pH buffer, yielded phage containing the consensus WRS. We also performed panning experiments on

Table 1. Phage selected from pannings on CD11c/CD18 and CD11b/CD18

Panning	Coated integrin	Phage library	Elution	Selected phage	
1, 2	CD11c/CD18	circular CL10	low pH	N1:	C-GRWSGWPADL-C
3	CD11c/CD18	circular CL10	EDTA	P8:	C-HKGHDRGKCR-C
4	CD11b/CD18	linear LL9	low pH	B1:	MDKTHFVNE
		circular CL10	CBRM1/29	E4:	C-PGGEWRKAK-C
5	CD11b/CD18	linear LL9	EDTA	AHK:	AHKSARKTE
		linear LL9	EDTA	W2:	WSYWETVAK

CD11b/CD18 bound to mAb LM2/1-Sepharose beads, resulting in the selection of phage with the sequence AHKSARKTE (AHK) and WSYWETVAK (W2). However, subsequent experiments failed to demonstrate specificity of such peptides.

Next, we compared binding of purified, selected phage with that of control phage F2 displaying a random amino acid sequence. Phage C-GRWSGWPADL-C (N1) bound approximately 5×10^3 -fold better to CD11c/CD18 than control phage F2, without binding to uncoated wells (Fig. 1A). We then investigated whether the affinity of the C-GRWSGWPADL-C phage was specific for the CD11c/CD18 integrin versus other $\beta 2$ -integrins. C-GRWSGWPADL-C was tested for binding to CD11b/CD18, yielding about 10-fold higher binding than control phage (Fig. 1B), which was minimal affinity relative to the 5×10^3 -fold difference observed with CD11c/CD18. These results suggest that binding of the C-GRWSGWPADL-C phage is specifically mediated by

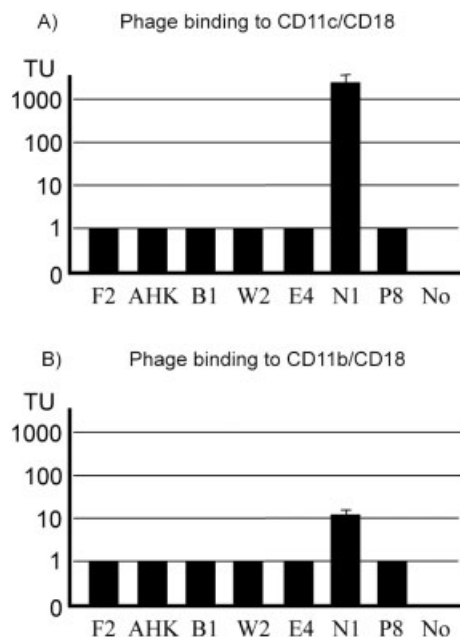


Figure 1. Binding of selected phage to purified CD11c/CD18 and CD11b/CD18. CD11c/CD18 (0.5 μ g/well)(A) or CD11b/CD18 (5 μ g/well)(B) was coated onto polysorb microtiter wells, washed and incubated with 10^8 TU of various purified phage. After intense washing, phage were eluted with low pH buffer and titers determined by plaque assay. Data were normalized to the binding of control phage F2 (set as 1). Phage C-GRWSGWPADL-C (N1) and C-HKGHDRGKKR-C (P8) were selected from panning on CD11c/CD18 and C-PGGEWRKAK-C (E4), MDKTHFVNE (B1), AHKSARKTE (AHK) and WSYWETVAK (W2) from panning on CD11b/CD18. A negative control, showing binding of C-GRWSGWPADL-C phage to polysorb microtiter wells in the absence of integrins, is indicated by No. Data represent mean \pm SD of the number of phage plaques on lawns of bacterial cells, determined from three independent experiments.

the peptide it displays, and this affinity appears to be specific for the CD11c/CD18 integrin.

Fibrinogen is unable to compete for binding of C-GRWSGWPADL-C phage to CD11c/CD18

To investigate whether the C-GRWSGWPADL-C phage competes with known ligands for $\beta 2$ integrins, binding of C-GRWSGWPADL-C to CD11c/CD18 was tested in the presence of various concentrations of the known ligand fibrinogen (Fig. 2). CD11c/CD18 was pre-incubated for 10 min with fibrinogen (100 pM to 10 μ M), followed by addition of 10^8 transducing units (TU) of C-GRWSGWPADL-C phage or F2 control phage. Fibrinogen did not affect C-GRWSGWPADL-C phage binding at any concentration tested (Fig. 2), suggesting distinct binding epitopes of C-GRWSGWPADL-C phage and fibrinogen on CD11c/CD18.

Synthetic peptide C-GRWSGWPADL-C binds specifically to CD11c/CD18

We then tested whether the synthetic peptide C-GRWSGWPADL-C was able to compete with C-GRWSGWPADL-C phage for binding to CD11c/CD18 in microtiter wells. Interestingly, the synthetic peptide was unable to prevent phage binding even at concentrations of 1 mM (not shown). Given the pentavalent nature of the phage-displayed peptides, it was conceivable that the monomeric peptide alone had relatively low affinity for CD11c/CD18, but the pentavalent format conferred increased avidity that ultimately resulted in a detectable difference in binding.

To test the possibility that the C-GRWSGWPADL-C peptide binds specifically to CD11c/CD18 but with

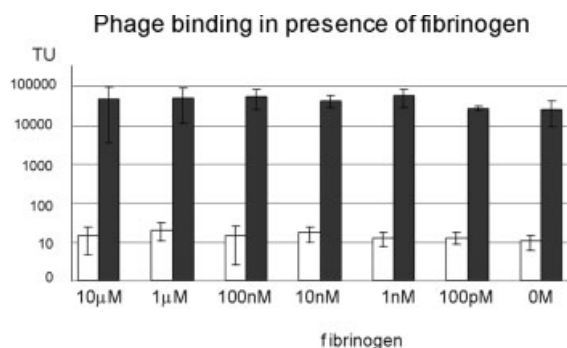


Figure 2. Effect of fibrinogen on the binding of purified C-GRWSGWPADL-C phage to CD11c/CD18. Wells coated with CD11c/CD18 (0.5 μ g/well) were incubated with various concentrations of fibrinogen for 10 min, followed by addition of 10^8 TU of C-GRWSGWPADL-C phage (■) or non-specific phage F2 (□) and further incubation for 2 hours. After extensive washing, phage was eluted with low pH buffer and titered. Data (mean \pm SD) were obtained from four independent experiments.

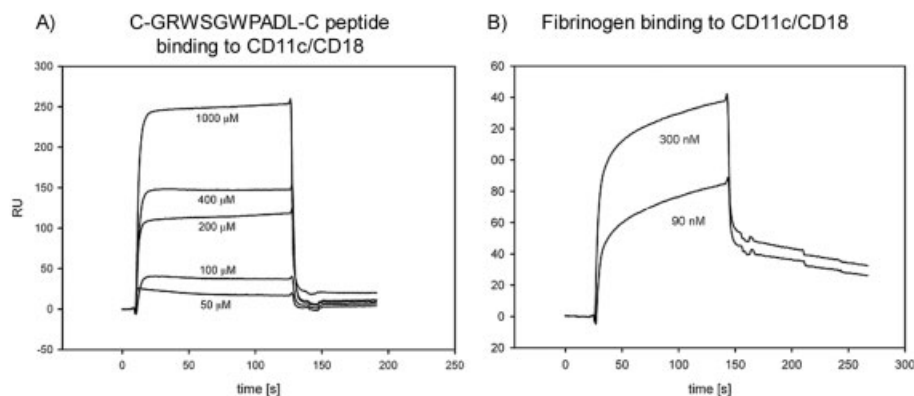


Figure 3. Binding of synthetic peptide C-GRWSGWPADL-C and fibrinogen to CD11c/CD18. Various concentrations of synthetic peptide C-GRWSGWPADL-C (A) or fibrinogen (B) were applied to CD11c/CD18 immobilized on CM5 BIAcore chips and binding was measured by surface plasmon resonance. Typical receptor-ligand binding curves were obtained. A K_D for synthetic peptide C-GRWSGWPADL-C of 56 μM and for fibrinogen of 23 nM was calculated using the BIAevaluation software.

relatively low affinity, surface plasmon resonance was performed on CM5 chip surfaces coated with purified CD11c/CD18, over which a solution containing various concentrations of synthetic peptide C-GRWSGWPADL-C (1.33 kDa), ranging from 50–1000 μM , was flowed at a constant rate. Peptide C-GRWSGWPADL-C bound to CD11c/CD18 (Fig. 3A), resulting in typical association and dissociation phases, whereby a K_D of 56 μM was calculated (Table 2). An irrelevant circular peptide and BSA served as controls and did not bind to CD11c/CD18 (not shown). Binding of peptide C-GRWSGWPADL-C was specific to CD11c/CD18, as no signal was detected with CD11b/CD18 coated chips. To verify the intactness of the purified CD11c/CD18, we measured binding of fibrinogen (340 kDa) (Fig. 3B) and obtained typical receptor-ligand binding curves, with association, saturation and dissociation phases. A K_D of 23 nM was determined (Table 2). The greater RU observed for peptide relative to fibrinogen binding to CD11c/CD18 is due to the greater contribution of buffer effect by the much higher concentration of synthetic peptide compared with that of fibrinogen. The changes in RU are due to a combination of buffer effect and association of the protein or peptide to the target protein coupled to the chip, which is proportional to the mass bound to the chip, whereby the calculation of the kinetic parameters

is adjusted for the buffer effect. These results demonstrate that monomeric C-GRWSGWPADL-C peptide binds specifically to CD11c/CD18, but the affinity of this interaction appears to be relatively low as compared to the pentavalent phage or the known ligand fibrinogen.

C-GRWSGWPADL-C phage binds specifically to monocytes

Since monocytes and NK-like lymphocytes express high levels of CD11c/CD18, binding of C-GRWSGWPADL-C phage to blood leukocytes was tested by flow cytometry. We observed a fluorescence intensity shift for monocytes (red) and a small subset of lymphocytes (green) after labeling with C-GRWSGWPADL-C phage (Fig. 4), consistent with the known pattern of CD11c/CD18 expression and indicating C-GRWSGWPADL-C phage binding to CD11c/CD18 expressing cells. In contrast, the main populations of lymphocytes, that do not express CD11c/CD18, did not shift after incubation with C-GRWSGWPADL-C phage. We next tested whether synthetic C-GRWSGWPADL-C peptide inhibits C-GRWSGWPADL-C phage binding to monocytes and NK-like subsets of lymphocytes. Neither 1 mM C-GRWSGWPADL-C peptide nor control peptide inhibited

Table 2. Binding of synthetic peptide C-GRWSGWPADL-C and fibrinogen to CD11c/CD18^{a)}

Immobilized ligand	Analyte	k_a $\text{M}^{-1}\text{s}^{-1}$	k_d s^{-1}	K_D M
CD11c/CD18	synthetic peptide			
	CGRWSGWPADLC	4.6×10^1	2.6×10^{-3}	5.6×10^{-5}
CD11c/CD18	fibrinogen	1.7×10^5	3.7×10^{-3}	2.3×10^{-8}

^{a)} CD11c/CD18 was immobilized on CM5 chips, and binding of synthetic peptide C-GRWSGWPADL-C and fibrinogen was determined by surface plasmon resonance (BIAcore).

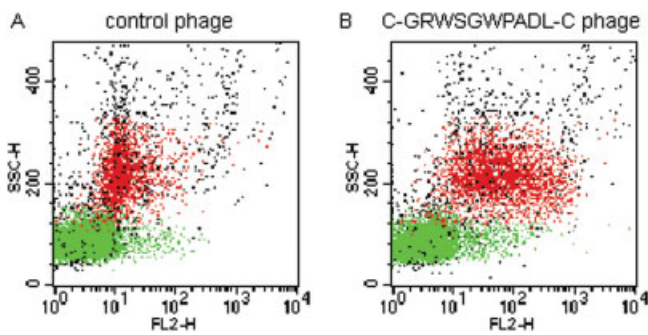


Figure 4. Binding of C-GRWSGWPADL-C phage to blood mononuclear cells. Monocytes (red squares) and lymphocytes (green squares) were isolated from healthy volunteers. Binding of control phage (A) and C-GRWSGWPADL-C phage (B) was analyzed in flow cytometric analyses. Cell-bound phage were detected with biotinylated anti-M13 phage antibody followed by secondary antibody PE-streptavidin.

binding of C-GRWSGWPADL-C phage (not shown). The ability of anti-CD11c antibody 4G1, a partial functional blocker of CD11c/CD18, to inhibit C-GRWSGWPADL-C phage binding was tested in flow cytometry analyses (Fig. 5). Neither antibody 4G1 nor control anti-CD14 antibody inhibited C-GRWSGWPADL-C phage binding to both cell types (Fig. 5A and B). Nonetheless, co-staining with antibody 4G1 and C-GRWSGWPADL-C

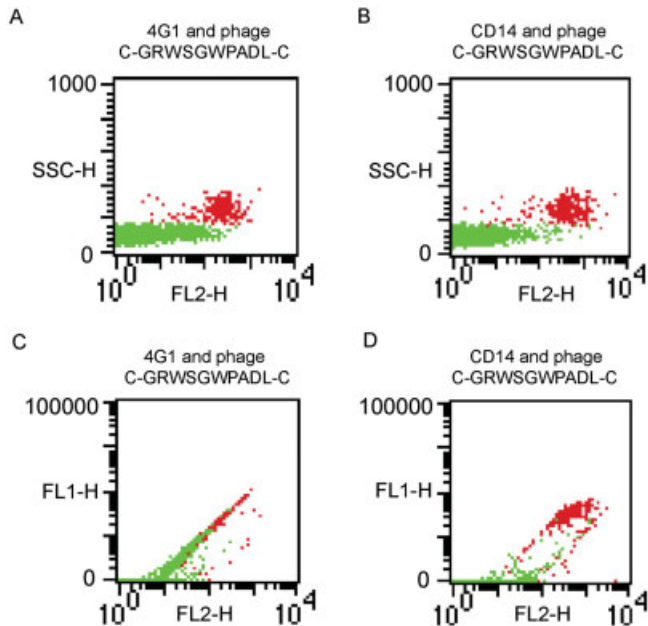


Figure 5. C-GRWSGWPADL-C phage and anti-CD11c antibody 4G1 bind to non-overlapping sites on CD11c/CD18. C-GRWSGWPADL-C phage binding to monocytes (red squares) and a subset of lymphocytes (green squares) was investigated in the presence of the functional CD11c/CD18-blocker antibody 4G1 (A), or anti-CD14 control antibody (B). Simultaneous incubation and co-labeling of antibody 4G1 and C-GRWSGWPADL-C phage (C) or anti-CD14 control antibody and C-GRWSGWPADL-C phage (D).

phage (Fig. 5C) demonstrates proportional co-labeling intensities, consistent with the ligands labeling non-overlapping sites on the same cell surface molecule, *i.e.* CD11c/CD18. In contrast, in a control analysis with anti-CD14 antibody and C-GRWSGWPADL-C phage, there was no proportionality to co-labeling, although the anti-CD14 antibody was clearly bound. This control further confirms that the co-labeling pattern seen in Fig. 5C is not merely an artefact of poor compensation by the cytometer.

ICAM-1 binds to CD11c/CD18 and competes for binding of C-GRWSGWPADL-C phage to CD11c/CD18

A database search with the C-GRWSGWPADL-C sequence revealed a similar linear sequence in the fifth domain of ICAM-1 and an alternative, phase-shifted alignment in domain D4 (see the Discussion section for detailed information). To test the hypothesis that the selected phage motif mimics a region on ICAM-1, we first confirmed direct binding of CD11c/CD18 to ICAM-1 by surface plasmon resonance. A fusion protein of the extracellular moiety of ICAM-1 and Fc (ICAM-1/Fc) was immobilized on a CM5 BIAcore chip and various concentrations of CD11c/CD18 were applied to assess binding properties (Fig. 6A). The specific binding of CD11c/CD18 to ICAM-1 was indicated by typical binding curves with association and dissociation phases. A K_D of 3.9 μM was determined (Table 3). Immobilized ICAM-1/Fc was also incubated with various concentrations of CD11b/CD18 (Fig. 6B). Specific binding curves were observed and a K_D of 680 nM was determined.

Having demonstrated that ICAM-1 directly binds to CD11c/CD18, we performed a competition assay for the binding of fusion protein ICAM-1/Fc and C-GRWSGWPADL-C phage to CD11c/CD18 (Fig. 7). ICAM-1/Fc efficiently prevented binding of C-GRWSGWPADL-C phage to CD11c/CD18. Nonspecific binding of a wild-phage was not affected by ICAM-1/Fc. Binding of C-GRWSGWPADL-C phage and wild-phage to CD11c/CD18 in the presence of Fc alone was similar to that in the absence of ICAM-1/Fc. In control experiments where wells were coated with BSA instead of CD11c/CD18, neither wild-phage nor C-GRWSGWPADL-C phage showed significant binding.

Evidence for interaction of CD11c/CD18 with the site in domain D4 of ICAM-1

Since the selected phage motif C-GRWSGWPADL-C may mimic the linear GNWTWP sequence in domain D5 or the phase-shifted PEDNGRSFS epitope in domain D4 of ICAM-1, we constructed mutant ICAM-1/Fc-fusion proteins containing either the full-length extracellular

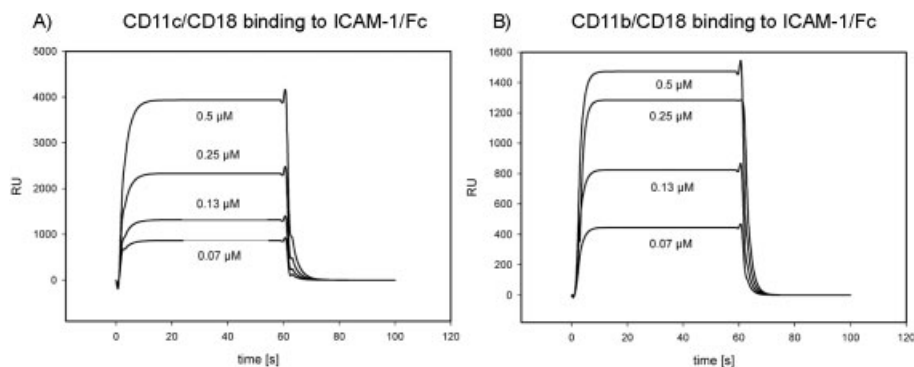


Figure 6. Binding of CD11c/CD18 and CD11b/CD18 to ICAM-1 measured with surface plasmon resonance. ICAM-1/Fc was coated on CM5 BIAcore chips, and various concentrations of CD11c/CD18 (A) or CD11b/CD18 (B) were applied. Curves typical for receptor-ligand interactions were observed with a K_D for CD11c/CD18 of $3.9 \mu\text{M}$ and for CD11b/CD18 of 680 nM .

Table 3. Binding of ICAM-1 to CD11c/CD18 and CD11b/CD18^{a)}

Immobilized	Analyte	k_a	k_d	K_D
ligand		$\text{M}^{-1}\text{s}^{-1}$	s^{-1}	M
ICAM-1/Fc	CD11c/CD18	1.2×10^5	4.9×10^{-1}	3.9×10^{-6}
ICAM-1/Fc	CD11b/CD18	8.8×10^5	6.0×10^{-1}	6.8×10^{-7}

^{a)} ICAM-1/Fc was immobilized on CM5 chips, and binding of CD11c/CD18 and CD11b/CD18 was measured by surface plasmon resonance (BIAcore).

domain (ICAM-1 D1–5), the extracellular domain missing D5 (ICAM-1 D1–4) or missing both D4 and D5 (ICAM-1 D1–3) (Fig. 8A). Using a nitrocellulose-based assay, we demonstrated the binding of ICAM-1 D1–5 to CD11c/CD18. The synthetic circular peptide C-

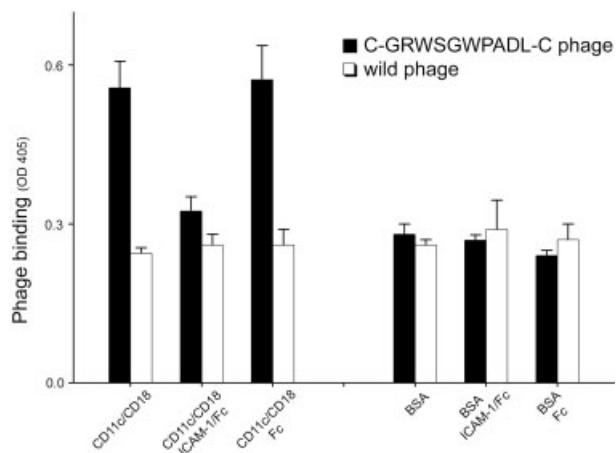


Figure 7. ICAM-1/Fc prevents binding of C-GRWSGWPADL-C phage to CD11c/CD18. Binding of C-GRWSGWPADL-C phage and wild-phage to CD11c/CD18 or BSA coated onto microtiter plate wells was determined in the presence or absence of ICAM-1/Fc or Fc control. After extensive washing, bound phage was detected by immunoassay using anti-M13 phage antibody, followed by color development and OD measurement at 405 nm. Black bars, C-GRWSGWPADL-C phage; white bars, wild-phage.

GRWSGWPADL-C abolished binding of ICAM-1/Fc to CD11c/CD18 at concentrations above $100 \mu\text{M}$ (Fig. 8B), although it failed to displace C-GRWSGWPADL-C phage from CD11c/CD18. We then compared the binding of full-length and mutant ICAM-1 constructs to CD11c/CD18 and observed comparable binding of ICAM-1 D1–5 and ICAM-1 D1–4, whereas ICAM-1 D1–3 almost completely lost its ability to bind to CD11c/CD18 (Fig. 8C). These findings demonstrate that domain D4 is essential for interaction with CD11c/CD18. The Fc fragment alone was applied as a control to assess unspecific binding. To verify the functionality of the ICAM-1 D1–3 construct, we determined whether it retained its ability to bind to CD11b/CD18, which was shown to interact with ICAM-1 in domain D3 [18]. Comparable binding of the full-length and both deletion constructs to CD11b/CD18 was observed (Fig. 8D), indicating that the lack of binding of ICAM-1 D1–3 to CD11c/CD18 was not due to improper folding of the construct.

Discussion

Interactions between ICAM and $\beta 2$ -integrins are complex. While it was shown that CD11a/CD18 binds to the first domain of all five known ICAM [14, 17, 20–22], CD11b/CD18 was found to bind to ICAM-1 at domain D3 [18], to ICAM-2 at D1 [13] and to ICAM-4 at a site

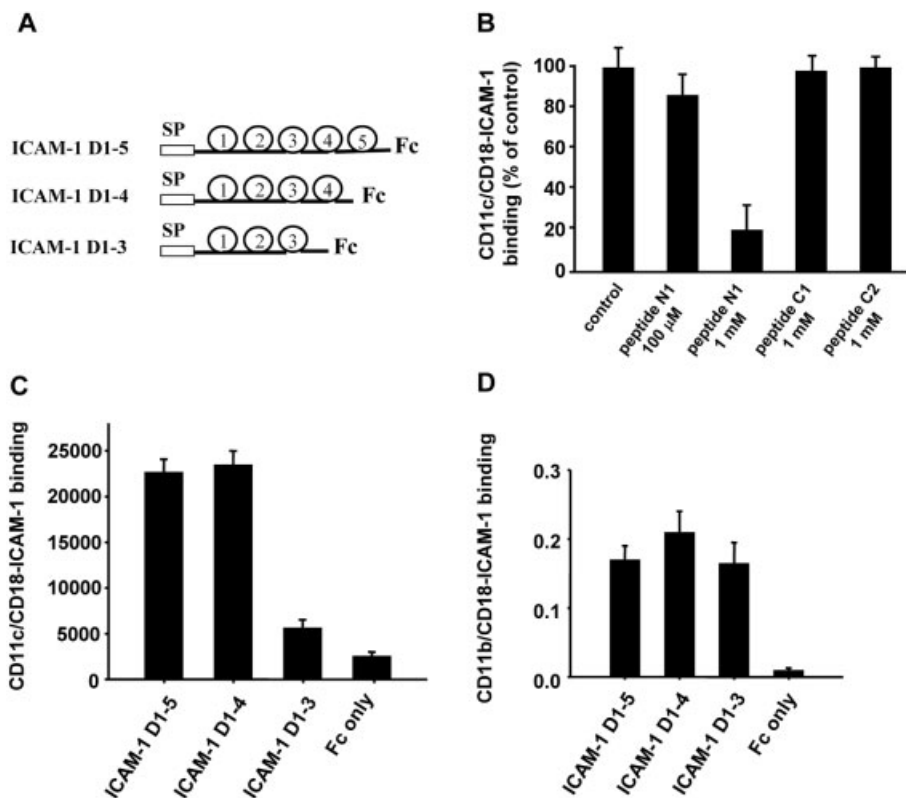


Figure 8. Domain D4 of ICAM-1 is essential for binding to CD11c/CD18. (A) Constructs for expression of fusion proteins between a modified region of rabbit IgG1-Fc and the extracellular moiety of wild-type and mutant ICAM-1. SP, signal peptide; ICAM-1 D1-5, wild-type extracellular moiety of ICAM-1; ICAM-1 D1-4, deletion of domain D5; ICAM-1 D1-3, deletion of domain D4 and D5. (B) Dot blot assay of nitrocellulose-immobilized CD11c/CD18 incubated with ICAM-1/Fc in the absence or presence of synthetic peptides. Data were normalized to the control in absence of peptide. N1, peptide C-GRWSGWPADL-C; C1, control peptide ELRGDMAAL; C2, control peptide C-MHNRHPMIKH-C. (C) Dot blot assay of CD11c/CD18 incubated with wild-type and mutant ICAM-1 constructs. Fc without fusion to ICAM-1 (Fc only) served as a control. Units correspond to chemiluminescence signal. (D) Microtiter-based assay of immobilized CD11b/CD18 incubated with wild-type and mutant ICAM-1/Fc constructs and Fc control. Units correspond to OD₄₀₅. Means \pm SD of four experiments are shown.

involving D1 and D2 [14]. ICAM-3 did not interact with CD11b/CD18 or CD11c/CD18 [19] but specifically bound CD11d/CD18 [23]. Although Diamond *et al.* [2] provided evidence that CD11c/CD18 binds to ICAM-1, by showing binding to purified ICAM-1 of Chinese hamster ovary (CHO) cells transfected with wild-type CD11c/CD18, direct binding with purified proteins has never been reported. Using surface plasmon resonance we now demonstrate the direct interaction between CD11c/CD18 and ICAM-1/Fc with a K_D of 3.9 μ M. Our findings of CD11c/CD18 binding with a lower affinity to ICAM-1 than CD11b/CD18 (K_D of 680 nM) are in line with findings from Diamond *et al.* [2], suggesting approximately fivefold higher binding to ICAM-1 of CD11b/CD18 transfected CHO cells compared with CD11c/CD18 transfected cells.

Applying phage-display technology, we selected a phage from the structurally constrained library CL10 bearing a circular peptide with the sequence C-GRWSGWPADL-C that binds selectively to CD11c/CD18. A database search revealed considerable similar-

ity between the circular peptide sequence C-GRWSGWPADL-C and the GNWTWP motif within the fifth domain of ICAM-1 (Fig. 9A). Moreover, Cys³⁷⁶ and Cys³⁹², encompassing the GNWTWP motif of ICAM-1, form a disulfide bridge [24], allowing a constrained conformation similar to that of the C-GRWSGWPADL-C peptide. Further experiments demonstrated that ICAM-1 competes with phage displaying this peptide for binding to CD11c/CD18 (Fig. 7). Together, these results suggested that the peptide C-GRWSGWPADL-C might mimic a functional epitope of ICAM-1.

To gain insight into potential location(s) of the phage selected C-GRWSGWPADL-C epitope within the ICAM-1 molecule, the crystal structure of ICAM-1 was modeled in software and motifs bearing similarity to the selected peptide were mapped onto this structure. According to the crystal structure, the GNWTWP motif of ICAM-1 resides in domain D5 (Fig. 9B, colored green), most proximal to the cell membrane and distant from the N-terminus. Although this motif represents a reasonable alignment of the C-GRWSGWPADL-C peptide with

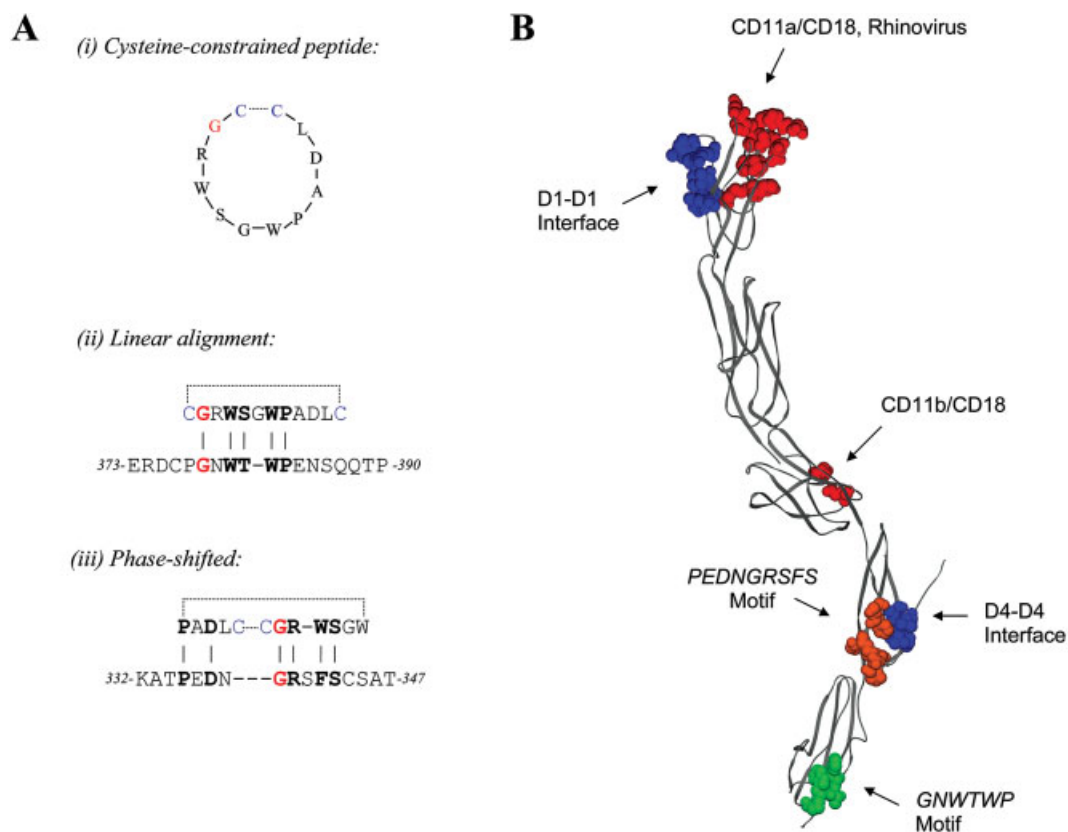


Figure 9. Functional epitopes of ICAM-1. (A) Alignment of the CD11c-selected peptide C-GRWSGWPADL-C with ICAM-1. (i) Illustration of the connectivity of the residues within the cysteine-constrained phage peptide. (ii) The simplest alignment is linear, based solely on primary structure. The first G of the peptide is aligned with the first residue of the ICAM-1 consensus. The cysteines are shown flanking this sequence. (iii) Phase-shifted alignment of the "circular" peptide: the first G corresponds to the fifth residue of the ICAM-1 consensus. (B) The ectodomain of ICAM-1 rendered as a ribbon structure with putative functional epitopes colored in space-filled representation. Residues implicated in binding to CD11a/CD18, CD11b/CD18, and rhinoviruses are colored red [25]. Residues implicated in cis-homodimer formation via D1 and D4 are colored blue [24, 25]. Two motifs that resemble the CD11c/CD18-selected phage are colored green and orange, corresponding to alignments (i) and (ii). D337, R340, and F342 of the PEDNGRSFS motif (orange) also contribute to the adjacent D4-D4 dimer interface (blue). This model suggests that ICAM-1 may bind to CD11c/CD18 via domains D4-D5, and this differs from ICAM-1 binding to other integrins and viral proteins via D1 and D3.

ICAM-1, it may not be accessible to ligands on opposing cells, an assumption supported by the finding that an ICAM-1 mutant lacking domain D5 is able to interact with CD11c/CD18 in a manner indistinguishable to that of full-length extracellular ICAM-1 (Fig. 8C).

We therefore sought to investigate alternative alignments for the C-GRWSGWPADL-C peptide that might produce epitopes more distal from the membrane and in areas already known to be involved in protein-protein interaction. Since the cysteine-constrained peptide is circular, alignments can be performed using any of the twelve residues as the origin (Fig. 9A). The simplest alignment is the linear GNWTWP alignment, where the first residue of the peptide corresponds to the first residue of the consensus on ICAM-1 (Fig. 9Aii). In contrast, in the phase-shifted alignment (Fig. 9Aiii), the first residue of the peptide corresponds to the fifth residue of the consensus motif. According to the crystal structure, this phase-shifted alignment corresponds to

the PEDNGRSFS motif in domain D4 (Fig. 9B, orange residues), more distal from the membrane than the GNWTWP epitope; thus it may be more accessible to interactions with adjacent cells. This epitope includes residues Asp³³⁷, Arg³⁴⁰, and Phe³⁴², which are part of the D4-D4 dimer interface [24]. Moreover, there is evidence for conformational changes in domain D4 between monomeric and dimeric form. Thus, the PEDNGRSFS epitope represents a reasonable binding site given its further distance from the membrane and that it contains residues known to be involved in protein-protein interactions. It is also distinct from the binding sites of CD11a/CD18 and rhinovirus, which are located in the N-terminal D1 domain [25] and the CD11b/CD18 binding site in domain D3 [24] (Fig. 9B, red residues). Most importantly, we demonstrated that the deletion of domain D4 and D5 of ICAM-1, but not of D5 alone, almost completely abolished interaction with CD11c/CD18, whereas interaction with CD11b/CD18 requiring

domain D3 was unaffected. Together, these findings are consistent with D4 being the CD11c/CD18 binding domain and suggest that the C-GRWSGWPADL-C phage mimics the PEDNGRSFS motif of ICAM-1.

A comparison of the PEDNGRSFS sequence in D4 of ICAM-1 with the corresponding sequences of ICAM-3 and ICAM-5 shows replacement of proline by negatively charged glutamate and of serine at the end of the motif by a bulky hydrophobic phenylalanine in the latter two proteins. Furthermore, in ICAM-1 the conserved aspartate is flanked by glutamate and asparagine while ICAM-3 and ICAM-5 have polar, uncharged serine and asparagines and negatively charged aspartate residues at these positions. These differences may explain the lack of interaction of CD11c/CD18 with ICAM-3 reported earlier [19]. In contrast, ICAM-2 and ICAM-4 contain only the first two Ig-like domains, and a motif with high similarity to the PEDNGRSFS motif was not found. Whether ICAM-2 and ICAM-4 interact with CD11c/CD18 remains to be investigated.

Our results indicate that multimeric display of five copies of C-GRWSGWPADL-C peptide attached to the pIII protein at the tip of the phage is critical for high affinity binding to CD11c/CD18. The monomeric synthetic peptide C-GRWSGWPADL-C was unable to displace C-GRWSGWPADL-C phage from purified CD11c/CD18 or from monocytes expressing high levels of CD11c/CD18. This failure to compete may be explained by differences in the conformation of free and phage-bound peptide ligand or by the increased avidity with five copies displayed at the tip of the phage. Domain D1 and D2 [25] as well as D3 to D5 [24] of ICAM-1 were crystallized, clearly suggesting that dimerization of ICAM-1 is mediated through D4 [24]. According to the 3D-structure, the D4 domain is exposed for potential ligand binding in this conformation, allowing dimeric display of the PEDNGRSFS motif. This supports our hypothesis that multimeric display of the motif might be essential for high affinity binding to CD11c/CD18. Accordingly, the K_D of 3.9 μM for dimeric ICAM-1/Fc was significantly lower than the K_D of 56 μM obtained for monomeric synthetic peptide C-GRWSGWPADL-C. The K_D of monomeric ICAM-1 was not determined in the present study and its affinity to bind to CD11c/CD18 may be much lower than that of the dimer. Although the monomeric synthetic peptide was unable to displace the pentavalent C-GRWSGWPADL-C phage from CD11c/CD18, incubation with high concentrations of the peptide abolished binding of ICAM-1/Fc to CD11c/CD18, supporting the evidence that the C-GRWSGWPADL-C peptide mimics the PEDNGRSFS motif on ICAM-1 and that this site mediates interaction with CD11c/CD18.

Integrins are binding receptors, which can switch between active and inactive conformations. Vorup-

Jensen *et al.* [26] reported a K_D of ligand iC3b of 400 μM for the binding to CD11c/CD18 in a surface plasmon resonance protein interaction experiment. A mutation, causing a conformational change in the I-domain C-terminal helix, increased the affinity to 2.4 μM . This K_D is in the range of that obtained for the binding of ICAM-1 to CD11c/CD18 in our experiment, suggesting that CD11c/CD18 existed in an active conformation on the CM5 chip. Binding of C-GRWSGWPADL-C phage to CD11c/CD18 could not be assessed by surface plasmon resonance, possibly due to the large size of the phage (900 nm) preventing it to fully protrude into the diffusion area of the chip and allow binding to the coated CD11c/CD18.

We also demonstrated that C-GRWSGWPADL-C phage specifically binds to monocytes known to express high levels of CD11c/CD18. Neither fibrinogen nor antibody 4G1, a partial CD11c/CD18 blocker recognizing the α -subunit (CD11c), were able to inhibit C-GRWSGWPADL-C phage binding, indicating that the ICAM-1 binding epitope on CD11c/CD18 is likely distinct from the epitope recognized by fibrinogen and antibody 4G1. Stacker and Springer [6] localized the binding site for antibody 4G1 between the third divalent cation binding domain and the C terminus on CD11c. The simultaneous detection of the binding of C-GRWSGWPADL-C phage and antibody 4G1 to monocytes expressing CD11c/CD18 suggests that they bind to non-overlapping sites on CD11c/CD18.

In conclusion, we have identified a peptide ligand, C-GRWSGWPADL-C, mediating specific binding to the β 2-integrin CD11c/CD18. We defined the binding site on CD11c/CD18 to be distinct from that of fibrinogen and antibody 4G1. Phage displaying the C-GRWSGWPADL-C motif were efficiently displaced from CD11c/CD18 by ICAM-1, which directly interacts with CD11c/CD18. Unlike CD11a/CD18 and CD11b/CD18 that interact with domain D1 and D3, respectively, we provide evidence for interaction of CD11c/CD18 with domain D4 of ICAM-1. Therefore, domain D4 represents an important area for study of leukocyte interactions and development of reagents that modulate such processes.

Materials and methods

Purification of CD11b/CD18 and CD11c/CD18

CD11b/CD18 was purified from PMN preparations as previously described [27–29]. Briefly, approximately 10^{10} neutrophils were solubilized in lysis buffer containing Triton X-100, and the precleared lysate was passed over a 6-mL immunoaffinity column (mAb-LM2/1 Sepharose), followed by washing and detergent exchange to 1% octylglucoside. Bound CD11b/CD18 was eluted with 50 mM triethylamine pH 10.5, 2 mM MgCl_2 and 1% octylglucoside followed by neutralization

and storage at -80°C . Typical yield was 1–2 mg per 10^{10} neutrophils. Purity was assessed by SDS-PAGE revealing two Coomassie stained bands of 170 and 95 kDa. Purification of CD11c/CD18 was performed as detailed by Staunton *et al.* [17]. Briefly, 30 g of human spleen, removed during treatment for hairy cell leukemia, was solubilized in 200 mL lysis buffer and the precleared lysate passed over an mAb 4G1-immunoaffinity column. After washing and detergent exchange, bound CD11c/CD18 was eluted with 50 mM triethylamine pH 11.5, 2 mM MgCl_2 and 1% octylglucoside, followed by neutralization and storage at -80°C . Typical yield was approximately 500 μg of purified protein consisting of two protein bands of 150 and 95 kDa in Coomassie stained SDS-PAGE. By ELISA, purified CD11c/CD18 was strongly reactive with anti-CD11c mAb 4G1, SHCL3 and anti-CD18 mAb TS1/18 but not with anti-CD11a mAb TS1/22 or anti-CD11b mAb 44a or CBRM1/29 (not shown). Furthermore, human intestinal epithelial cells (T84) specifically bound to immobilized CD11c/CD18 in a manner that was inhibited by anti-CD11c and anti-CD18 but not by anti-CD11a or anti-CD11b (not shown).

Screening of phage-display peptide libraries

Purified CD11c/CD18 or CD11b/CD18, diluted in HANKS buffered salt solution, pH 7.4, was coated onto polysorb 96-well microtiter plates (0.5 $\mu\text{g}/\text{well}$) (NUNC-Immuno Plate, Invitrogen, Carlsbad, CA) for 2 h at 37°C . Wells were washed with incubation buffer (HANKS, pH 7.4, containing 0.1% heat inactivated BSA and 0.05% octylglucoside), followed by blocking with 1% heat inactivated BSA. Separate panning experiments were performed using CD11b/CD18 bound at high density to Sepharose beads, covalently coupled to the non-inhibitory anti-CD11b mAb LM2/1. Incubation was for 4 h at 4°C , followed by washing twice with incubation buffer and six times with HANKS buffer containing 0.2% octylglucoside. Biopanning in microtiter wells was performed in a total volume of 100 μL and panning on beads in 1 mL containing 10^{10} TU of previously characterized phage libraries displaying either random decapeptides with a structural constraint imposed by a disulfide bond between two cysteine residues flanking the variable region (CL10), or displaying linear random nonapeptides (LL9) [30]. In experiments 1 and 2, bound phage were eluted with 0.9% NaCl, 100 mM glycine, pH 2.2, followed by neutralization of pH by adding 100 μL of 200 mM sodium bicarbonate, pH 7.4. In experiments 3 and 5, bound phage were eluted with 100 μL of 20 mM sodium-EDTA, pH 7.4, and in experiment 4 by adding 0.2 μg of anti-CD11b/CD18 antibody CBRM1/29. Eluted phage were amplified in K91 *Escherichia coli* as described [31]. An aliquot of 10^{10} TU was reapplied in a subsequent round of panning. After the fourth or fifth round of panning, the sequence of the peptide displayed by individual phage clones was determined.

Phage binding assay

Purified CD11c/CD18 (0.5 $\mu\text{g}/\text{well}$) or CD11b/CD18 (5 $\mu\text{g}/\text{well}$) coated onto microtiter wells were incubated with 10^8 TU of the corresponding phage for 4 h at 4°C . After extensive washing with HANKS buffer, pH 7.4, containing 0.05%

octylglucoside, bound phage were eluted with 100 μL of 0.9% NaCl, 100 mM glycine, pH 2.2, followed by neutralization of pH. Phage titer was determined by plaque assay as described earlier [32]. Data (mean \pm SD) were obtained from four independent experiments.

Competition experiments involving C-GRWSGWPADL-C phage binding to CD11c/CD18

Purified CD11c/CD18 (0.5 $\mu\text{g}/\text{well}$) was pre-incubated for 10 min at 25°C with various concentrations of fibrinogen (100 pM to 10 μM) or synthetic peptide C-GRWSGWPADL-C (100 pM to 100 μM), followed by incubation with phage (10^8 TU) for 2 h at 4°C . After extensive washing, bound phage were eluted and phage titer was determined by plaque assay. Data (mean \pm SD) were obtained from three independent experiments.

In competition assays using a fusion protein of Fc and the extracellular moiety of ICAM-1 (recombinant human ICAM-1/Fc, R&D Systems Inc. Minneapolis, MN), microtiter plate wells were coated with CD11c/CD18 (0.5 $\mu\text{g}/\text{well}$) and blocked with 1% heat inactivated BSA, followed by addition of 10^{11} phage particles in the presence or absence of purified ICAM-1/Fc or Fc control protein in blocking buffer. Alternatively, synthetic peptides (Chiron Technologies, Clayton, Victoria, Australia; purity $\geq 90\%$) were applied instead of ICAM-1/Fc. After 2 h at 37°C , wells were washed, probed with anti-phage antibody, developed colorimetrically and OD_{405} measured.

Surface plasmon resonance

Surface plasmon resonance experiments were performed on a BIAcore-2000 apparatus using CM5 chips with continuous flow of HANKS, pH 7.4, containing 1% octylglucoside. The surface of CM5 chips was activated by injecting 50 μL of *N*-hydroxylsuccinimide/*N*-hydroxylsuccinimide (NHS) and 1-ethyl-3-(3-dimethylaminopropyl) carbodiimide (EDC) with a flow rate of 5 $\mu\text{L}/\text{min}$, resulting in a baseline of approximately 13 000 RU. Activated chips were then coated with 30 μL of 0.0063 mg/mL purified CD11c/CD18 or 20 μL of 0.063 mg/mL ICAM-1/Fc in 50 mM potassium acetate, pH 5.0, 2 mM MgCl_2 , 2 mM CaCl_2 , and 1% octylglucoside, by injection with a flow rate of 5 $\mu\text{L}/\text{min}$, giving a signal increase of about 5000 RU for CD11c/CD18 and 350 RU for ICAM-1/Fc, respectively. Excess reactive groups were deactivated by injecting 30 μL of 1 M ethanolamine, pH 9.0, within 6 min. In a typical experiment, various concentrations of ligands diluted in HANKS buffer, pH 7.4, containing 1% octylglucoside were analyzed with a flow rate of 5 $\mu\text{L}/\text{min}$, giving an association and dissociation time of 2 min each. Interacting proteins were released from CD11c/CD18 on the CM5 chip with buffer TAE (40 mM Tris(hydroxymethyl)aminomethan, 50 mM acetic acid, 1 mM EDTA, adjusted with NaOH to pH 11.5) containing 1% octylglucoside.

Data analysis was performed using BIAevaluation version 3.1 software (BIAcore). All analyzed interactions were assumed to follow pseudo-first order kinetics. Calculated association (k_a) and dissociation (k_d) rates were derived by fitting the biosensor curves. K_D was calculated from the relation $K_D = k_d/k_a$. The presence of traces of multimers,

which might cause an overestimation of affinities, cannot be excluded.

Flow cytometry

Human mononuclear blood cells were isolated from healthy volunteers and flow cytometric immunophenotyping was performed as described [33, 34]. Cells were analyzed on a FACSort cytometer (Becton Dickinson, San Jose, CA). At least 10 000 events were measured. Data acquisition and analysis were accomplished using Cellquest software, version 3.1 (Becton Dickinson). Standard criteria were used for placing gates on different hematopoietic cell populations.

M13-phage was detected using anti-M13-biotin antibody (Serotec Inc, Raleigh, NC) and streptavidin-PE antibody (Jackson Laboratories, Bar Harbor, ME). CD11c/CD18 was detected with mouse anti-CD11c/CD18 mAb 4G1 [6] and Alexa-488 anti-mouse IgG antibody (Molecular Probes, Eugene, OR). CD14 was detected with a mouse mAb (BD PharMingen, San Diego, CA) and the same secondary antibody.

Preparation of recombinant chimeric ICAM-1/Fc

Soluble recombinant ICAM-1 proteins consisting of various extracellular domains of ICAM-1 (Fig. 8A) were prepared as described [35]. Human ICAM-1 was amplified by PCR from a human leukocyte cDNA library (Clontech, Palo Alto, CA) using the primer 5'-atctaagcttgcaccATGGCTCCCAGCAGCCCCGGC-3' in combination with 5'-aatagatccCACGGTCACCTCGCGGTGACC-3' (domains D1–5), 5'-aatagatccCTGGTTCCTGTGTATAAGCTGGC-3' (domains D1–4) or 5'-aatagatccCACTGTCTGCAGTGTCTCTGG-3' (domains D1–3). The cDNA products of ICAM-1 extracellular domains including a signal peptide were then fused to a cDNA encoding a modified region of rabbit IgG1-Fc, cloned into pcDNA3.1 (Invitrogen) and expressed in COS-7 cells. Secreted ICAM-1/Fc proteins were affinity-purified by Protein A-Sepharose resin (Sigma, St. Louis, MO), concentrated and dialyzed [35].

Binding of wild-type and mutant ICAM-1/Fc to CD11c/CD18 and CD11b/CD18

Microtiter-based assay

Purified CD11c/CD18 and CD11b/CD18 were immobilized in 96-well microtiter plates (3 µg/well, 4°C, overnight) and blocked with 1% BSA [29]. Microtiter plates coated with BSA only served as controls. Various ICAM-1/Fc chimeras or purified, recombinant rabbit Fc fragment derived from the vector used to produce the fusion protein (Fc-only) were added to wells (5 µg) and incubated for 1 h at 37°C. After three washes, binding was detected using HRP-conjugated goat anti-rabbit Fc antibody followed by addition of substrate and assessment of color development in a microtiter plate reader (OD₄₀₅).

Nitrocellulose-based assay

Purified CD11c/CD18 (3 µg) was immobilized onto nitrocellulose sheets using a 96-well dot blot apparatus (Bio-Rad), blocked with HBSS containing 1% BSA and incubated with ICAM-1 chimera (5 µg/mL in blocking buffer) for 1 h at 37°C. After washing, bound ICAM-1 chimeras were detected after incubation with HRP-conjugated goat anti-rabbit Fc antibody using enhanced chemiluminescence. Densitometry of dot blots was performed and analyzed using USCAN-IT gel scanner software (Silk scientific Corporation, UT).

Modeling of the ICAM-1 crystal structure

The extracellular domain of ICAM-1 was modeled in the Swiss-PdbViewer (GlaxoSmithKline) using PDB# 1P53 for domains D3-D5 and PDB# 1IC1 for domains D1-D2. A composite structure for the entire D1-D5 region was rendered based on the model provided by Yang *et al.* [24].

Acknowledgements: We thank Cissy Geigerman and Ross E. Fuller, Emory University, Atlanta, for expert technical support and Dr. Ursula Hinz, Swiss-Prot, Geneva, for helpful discussion. This work was supported by grants to A.O. from the Clötta Research Foundation and the Swiss National Science Foundation (3100A0-100060) and by grants from the NIH to DLJ (DK60647) and C.A.P. (HL54229, HL72124, DK61379, CA91435).

References

- 1 Springer, T. A., Traffic signals on endothelium for lymphocyte recirculation and leukocyte emigration. *Annu. Rev. Physiol.* 1995. **57**: 827–872.
- 2 Diamond, M. S., Garcia-Aguilar, J., Bickford, J. K., Corbi, A. L. and Springer, T. A., The I domain is a major recognition site on the leukocyte integrin Mac-1 (CD11b/CD18) for four distinct adhesion ligands. *J. Cell Biol.* 1993. **120**: 1031–1043.
- 3 Ihanus, E., Uotila, L., Toivanen, A., Stefanidakis, M., Bailly, P., Cartron, J. P. and Gahmberg, C. G., Characterization of ICAM-4 binding to the I domains of the CD11a/CD18 and CD11b/CD18 leukocyte integrins. *Eur. J. Biochem.* 2003. **270**: 1710–1723.
- 4 Oxvig, C., Lu, C. and Springer, T. A., Conformational changes in tertiary structure near the ligand binding site of an integrin I domain. *Proc. Natl. Acad. Sci. USA* 1999. **96**: 2215–2220.
- 5 Harris, E. S., McIntyre, T. M., Prescott, S. M. and Zimmerman, G. A., The leukocyte integrins. *J. Biol. Chem.* 2000. **275**: 23409–23412.
- 6 Stacker, S. A. and Springer, T. A., Leukocyte integrin P150,95 (CD11c/CD18) functions as an adhesion molecule binding to a counter-receptor on stimulated endothelium. *J. Immunol.* 1991. **146**: 648–655.
- 7 Micklem, K. J. and Sim, R. B., Isolation of complement-fragment-iC3b-binding proteins by affinity chromatography. The identification of p150,95 as an iC3b-binding protein. *Biochem. J.* 1985. **231**: 233–236.
- 8 Altieri, D. C., Agbanyo, F. R., Plescia, J., Ginsberg, M. H., Edgington, T. S. and Plow, E. F., A unique recognition site mediates the interaction of fibrinogen with the leukocyte integrin Mac-1 (CD11b/CD18). *J. Biol. Chem.* 1990. **265**: 12119–12122.
- 9 Diamond, M. S., Alon, R., Parkos, C. A., Quinn, M. T. and Springer, T. A., Heparin is an adhesive ligand for the leukocyte integrin Mac-1 (CD11b/CD18). *J. Cell Biol.* 1995. **130**: 1473–1482.

- 10 Cai, T. Q. and Wright, S. D., Human leukocyte elastase is an endogenous ligand for the integrin CR3 (CD11b/CD18, Mac-1, alpha M beta 2) and modulates polymorphonuclear leukocyte adhesion. *J. Exp. Med.* 1996. **184**: 1213–1223.
- 11 Santoso, S., Sachs, U. J., Kroll, H., Linder, M., Ruf, A., Preissner, K. T. and Chavakis, T., The junctional adhesion molecule 3 (JAM-3) on human platelets is a counterreceptor for the leukocyte integrin Mac-1. *J. Exp. Med.* 2002. **196**: 679–691.
- 12 Zen, K., Babbin, B. A., Liu, Y., Whelan, J. B., Nusrat, A. and Parkos, C. A., JAM-C is a component of desmosomes and a ligand for CD11b/CD18-mediated neutrophil transepithelial migration. *Mol. Biol. Cell* 2004. **15**: 3926–3937.
- 13 Xie, J., Li, R., Kotovuori, P., Vermot-Desroches, C., Wijdenes, J., Arnaout, M. A., Nortamo, P. and Gahmberg, C. G., Intercellular adhesion molecule-2 (CD102) binds to the leukocyte integrin CD11b/CD18 through the A domain. *J. Immunol.* 1995. **155**: 3619–3628.
- 14 Hermand, P., Huet, M., Callebaut, I., Gane, P., Ihanus, E., Gahmberg, C. G., Cartron, J. P. and Bailly, P., Binding sites of leukocyte beta 2 integrins (LFA-1, Mac-1) on the human ICAM-4/LW blood group protein. *J. Biol. Chem.* 2000. **275**: 26002–26010.
- 15 Koivunen, E., Wang, B. and Ruoslahti, E., Phage libraries displaying cyclic peptides with different ring sizes: ligand specificities of the RGD-directed integrins. *Biotechnology (N Y)* 1995. **13**: 265–270.
- 16 Koivunen, E., Ranta, T. M., Annala, A., Taube, S., Uppala, A., Jokinen, M., van Willigen, G. et al., Inhibition of beta(2) integrin-mediated leukocyte cell adhesion by leucine-leucine-glycine motif-containing peptides. *J. Cell Biol.* 2001. **153**: 905–916.
- 17 Staunton, D. E., Dustin, M. L., Erickson, H. P. and Springer, T. A., The arrangement of the immunoglobulin-like domains of ICAM-1 and the binding sites for LFA-1 and rhinovirus. *Cell* 1990. **61**: 243–254.
- 18 Diamond, M. S., Staunton, D. E., Marlin, S. D. and Springer, T. A., Binding of the integrin Mac-1 (CD11b/CD18) to the third immunoglobulin-like domain of ICAM-1 (CD54) and its regulation by glycosylation. *Cell* 1991. **65**: 961–971.
- 19 de Fougères, A. R., Diamond, M. S. and Springer, T. A., Heterogenous glycosylation of ICAM-3 and lack of interaction with Mac-1 and p150,95. *Eur. J. Immunol.* 1995. **25**: 1008–1012.
- 20 Li, R., Nortamo, P., Valmu, L., Tolvanen, M., Huuskonen, J., Kantor, C. and Gahmberg, C. G., A peptide from ICAM-2 binds to the leukocyte integrin CD11a/CD18 and inhibits endothelial cell adhesion. *J. Biol. Chem.* 1993. **268**: 17513–17518.
- 21 Holness, C. L., Bates, P. A., Little, A. J., Buckley, C. D., McDowall, A., Bossy, D., Hogg, N. and Simmons, D. L., Analysis of the binding site on intercellular adhesion molecule 3 for the leukocyte integrin lymphocyte function-associated antigen 1. *J. Biol. Chem.* 1995. **270**: 877–884.
- 22 Tian, L., Nyman, H., Kilgannon, P., Yoshihara, Y., Mori, K., Andersson, L. C., Kaukinen, S. et al., Intercellular adhesion molecule-5 induces dendritic outgrowth by homophilic adhesion. *J. Cell Biol.* 2000. **150**: 243–252.
- 23 Van der Vieren, M., Le Trong, H., Wood, C. L., Moore, P. F., St John, T., Staunton, D. E. and Gallatin, W. M., A novel leukointegrin, alpha d beta 2, binds preferentially to ICAM-3. *Immunity* 1995. **3**: 683–690.
- 24 Yang, Y., Jun, C. D., Liu, J. H., Zhang, R., Joachimiak, A., Springer, T. A. and Wang, J. H., Structural basis for dimerization of ICAM-1 on the cell surface. *Mol. Cell* 2004. **14**: 269–276.
- 25 Casasnovas, J. M., Stehle, T., Liu, J. H., Wang, J. H. and Springer, T. A., A dimeric crystal structure for the N-terminal two domains of intercellular adhesion molecule-1. *Proc. Natl. Acad. Sci. USA* 1998. **95**: 4134–4139.
- 26 Vorup-Jensen, T., Ostermeier, C., Shimaoka, M., Hommel, U. and Springer, T. A., Structure and allosteric regulation of the alpha X beta 2 integrin I domain. *Proc. Natl. Acad. Sci. USA* 2003. **100**: 1873–1878.
- 27 Parkos, C. A., Colgan, S. P., Liang, T. W., Nusrat, A., Bacarra, A. E., Carnes, D. K. and Madara, J. L., CD47 mediates post-adhesive events required for neutrophil migration across polarized intestinal epithelia. *J. Cell Biol.* 1996. **132**: 437–450.
- 28 Parkos, C. A., Colgan, S. P., Diamond, M. S., Nusrat, A., Liang, T. W., Springer, T. A. and Madara, J. L., Expression and polarization of intercellular adhesion molecule-1 on human intestinal epithelia: consequences for CD11b/CD18-mediated interactions with neutrophils. *Mol. Med.* 1996. **2**: 489–505.
- 29 Zen, K., Liu, Y., Cairo, D. and Parkos, C. A., CD11b/CD18-dependent interactions of neutrophils with intestinal epithelium are mediated by fucosylated proteoglycans. *J. Immunol.* 2002. **169**: 5270–5278.
- 30 Mazzucchelli, L., Burritt, J. B., Jesaitis, A. J., Nusrat, A., Liang, T. W., Gewirtz, A. T., Schnell, F. J. and Parkos, C. A., Cell-specific peptide binding by human neutrophils. *Blood* 1999. **93**: 1738–1748.
- 31 Audige, A., Frick, C., Frey, F. J., Mazzucchelli, L. and Odermatt, A., Selection of peptide ligands binding to the basolateral cell surface of proximal convoluted tubules. *Kidney Int.* 2002. **61**: 342–348.
- 32 Odermatt, A., Audige, A., Frick, C., Vogt, B., Frey, B. M., Frey, F. J. and Mazzucchelli, L., Identification of receptor ligands by screening phage-display peptide libraries *ex vivo* on microdissected kidney tubules. *J. Am. Soc. Nephrol.* 2001. **12**: 308–316.
- 33 Jaye, D. L., Edens, H. A., Mazzucchelli, L. and Parkos, C. A., Novel G protein-coupled responses in leukocytes elicited by a chemotactic bacteriophage displaying a cell type-selective binding peptide. *J. Immunol.* 2001. **166**: 7250–7259.
- 34 Jaye, D. L., Nolte, F. S., Mazzucchelli, L., Geigerman, C., Akyildiz, A. and Parkos, C. A., Use of real-time polymerase chain reaction to identify cell- and tissue-type-selective peptides by phage display. *Am. J. Pathol.* 2003. **162**: 1419–1429.
- 35 Liu, Y., Nusrat, A., Schnell, F. J., Reaves, T. A., Walsh, S., Pochet, M. and Parkos, C. A., Human junction adhesion molecule regulates tight junction resealing in epithelia. *J. Cell Sci.* 2000. **113 (Pt 13)**: 2363–2374.